Int J Adv Manuf Technol
DOI 10.1007/s00170-012-3924-7

ORIGINAL ARTICLE

A look-ahead and adaptive speed control algorithm for high-speed CNC equipment

Lin Wang · Jianfu Cao

Received: 13 February 2011 / Accepted: 10 January 2012

Abstract A novel look-ahead and adaptive speed control algorithm is proposed. The algorithm improves the efficiency of rapid linking of feedrate for high-speed machining and avoids impact caused by acceleration gust. Firstly, discrete S-curve speed control algorithm is presented according to the principle of S-curve acceleration and deceleration. Secondly, constraints of linked feedrates are derived from several limits, including the axis feedrate and feed acceleration limits, the circular arc radius error limit, and the machining segment length limit. With these constraints, the optimal linked feedrate is sought to achieve the maximum feedrate by using look-ahead method. Since the actual ending velocity of machining segment equals to the corresponding optimal linked feedrate, speed control of each segment can be executed. Finally, the proposed algorithm is implemented in a pipe cutting CNC system, and experimental results show that the proposed algorithm achieves a high-speed and smooth linking feedrate and improvements in productivity and stationarity.

Keywords Discrete S-curve acceleration and deceleration · Look-ahead and adaptive speed optimization · Linked feedrate · High speed machining

L. Wang · J. Cao (✉)
State Key Laboratory for Manufacturing System Engineering, Xi'an Jiaotong University, Xi'an 710049, People's Republic of China
e-mail: cjf@mail.xjtu.edu.cn

L. Wang
e-mail: wanglin_05@163.com

Nomenclature

$a_{\Lambda\,\max}$	The maximum feed acceleration of axis Λ, $\Lambda = x, y, z$
a_j	The acceleration in the j-th interpolation period
$a_{\max}$	The maximum allowable acceleration of a segment denoted by $N_m = \lfloor a_{\max}/(j_{\max}T)\rfloor$
$a_{\max,h}$	The maximum allowable acceleration of $l(h)$ denoted by $N_{m,h} = \lfloor a_{\max,h}/(j_{\max}T)\rfloor$
e_R	The maximum radius error
$e_{\Lambda e,h}$	Component of $e_{e,h}$ in the Λ direction, $\Lambda = x, y, z$
$e_{\Lambda s,h+1}$	Component of $e_{s,h+1}$ in the Λ direction, $\Lambda = x, y, z$
$e_{e,h}$	The unit direction vector at the ending point of segment $l(h)$
$e_{s,h+1}$	The unit direction vector at the starting point of segment $l(h+1)$
F	The instruction feedrate of a segment
F_h	The instruction feedrate of segment $l(h)$
$j_{\max}$	The maximum allowable jerk
L_1	The displacement of acceleration process
L_2	The displacement of deceleration process
$L_{th}(\cdot)$	The theoretical displacement of the acceleration (deceleration) process
l	The segment length of a segment
l_h	The segment length of segment $l(h)$
$maxErr$	The maximum allowable displacement error
N	The number of the segments of a tool path
N_t	The maximum number of look-ahead segments
S_d	The length of deceleration region
T	The interpolation period

Published online: 17 February 2012

$V_{th}(\cdot)$	The actual ending velocity of the acceleration (deceleration) process
$v_{\Lambda\max}$	The maximum feedrate of axis Λ, $\Lambda = x, y, z$
v_e	The ending velocity of a segment
$v_{e,h}$	The linked feedrate between $l(h)$ and $l(h+1)$
$v^*_{e,h}$	The optimal linked feedrate between segments $l(h)$ and $l(h+1)$
$v_{e\max,h}$	The upper limit of $v_{e,h}$
$v^{(1)}_{e\max,h}$	The upper limit of $v_{e,h}$ with the axis feedrate limits
$v^{(2)}_{e\max,h}$	The upper limit of $v_{e,h}$ with the axis feed acceleration limits
v_j	The feedrate in the j-th interpolation period
v_m	The actual maximum feedrate of a segment
$v^{(arc)}_{\max}$	The upper limit of $v_{e,h}$ with the circular arc radius error limit
v_s	The starting velocity of a segment

1 Introduction

In order to deliver the rapid feed motion for high-speed machining, computer numerical control (CNC) equipment often needs to operate at a feedrate up to 40 m/min with acceleration up to 2 g [5]. To enhance the manufacturing accuracy and machining efficiency in high-speed circumstances, CNC equipment must have the abilities of high-precision multi-axial linkage interpolation, 3D cutter compensation, advanced positioning, and speed servo controlling. Among these characteristics, the speed control algorithm usually affects the machining efficiency, quality of parts, and longevity of cutter. Therefore, efficient speed control algorithm suitable for high-speed machining becomes very important for enhancing the performance of the CNC equipment.

Many researchers are working focusing on the field of speed control for high-speed machining. In [3, 6], an acceleration/deceleration (ACC/DEC) after interpolation method is presented for realizing high-speed machining of continuous small line blocks. However, the precise linkage relationship among different machining axes was hard to guarantee, thereby the machining accuracy decreased. In [7, 8, 10, 11, 18], several look-ahead speed control algorithms based on linear ACC/DEC are proposed. Because of the limitation of the linear ACC/DEC, a great impact of CNC equipment caused by acceleration gust still existed. The quality of parts and the longevity of the machine tools were influenced in these algorithms as well. To avoid the limitation of the linear ACC/DEC, NURBS curve-based algorithms [1, 4, 9, 12, 13, 15] and Bezier curve-based algorithms [16, 17] were proposed. However, most of the algorithms attempted to keep a constant feedrate without considering chord errors, and the computations were complex and difficult for hardware implementations. Moreover, some S-curve-based look-ahead algorithms were presented in [2, 19], yet the algorithms were derived based on the assumption of a continuous feedrate variation and could not be directly applied to real CNC systems due to the discretization of feedrate in real systems.

Based on the discrete S-curve ACC/DEC, a novel look-ahead and adaptive speed control algorithm is presented in this paper. Firstly, the uniform formulas of acceleration, feedrate, and displacement for both acceleration process and deceleration process are given, and then the discrete S-curve speed control algorithm is presented. With constraints of linked feedrates, which are derived from the axis feedrate and feed acceleration limits, the circular arc radius error limit, and the machining segment length limit, the optimal linked feedrate can be sought in the scope of maximum preprocessing segments. The number of the preprocessing segments can be adjusted automatically according to the transition of the segments. Given the actual ending velocity of machining segment equaling to the corresponding optimal linked feedrate, the speed control of each segment can be executed. The implementation of the proposed speed control algorithm for high-speed CNC equipment is also presented and applied to a six-axis pipe cutting CNC system to verify the efficiency. The experimental results show that the proposed algorithm can achieve a high-speed, smooth linking feedrate and thus meet the requirements of high-speed machining.

The paper is organized as follows: In Section 2, the discrete S-curve ACC/DEC algorithm is described, which gives the uniform recursive formulas of the acceleration rate, feedrate, and displacement. Section 3 presents the look-ahead and adaptive speed control algorithm, including linked feedrate constraints of S-curve ACC/DEC derivation, optimal linked feedrate pre-computation, and adaptive S-curve speed control of current segment. In Sections 4 and 5, the implementations of the proposed algorithm are carried out in a high-speed CNC system, and experimental results obtained are discussed. In Section 6, the conclusion is presented.

2 Discrete S-curve acceleration and deceleration

In order to avoid the limitation of the linear ACC/DEC, the S-curve ACC/DEC mode, which can ensure that

the acceleration is continuous by controlling the invariable jerk, is adopted in this paper. The kinematic profiles of S-curve ACC/DEC process are illustrated in Fig. 1. The process is usually divided into seven regions from region I to region VII, including accelerated acceleration, constant acceleration, decelerated acceleration, constant velocity, accelerated deceleration, constant deceleration, and decelerated deceleration [5, 19].

The symbols of Fig. 1 are defined as follows: t denotes the absolute time; $t_1, t_2, \ldots, t_7$ denote the time boundaries of each region; $s_k(k = 1, 2, \ldots, 7)$ denotes the displacement reached at the end of the k-th region; v_s denotes the starting velocity; F denotes the instruction feedrate; v_e denotes the ending velocity; $v_k(k = 1, 2, \ldots, 7)$ denotes the feedrate reached at the end of the k-th region; A and D denote the acceleration and deceleration magnitudes at regions II and VI, respectively; J_1, J_3, J_5, and J_7 denote the magnitudes of jerk in regions I, III, V, and VII; $T_k(k = 1, 2, \ldots, 7)$ denotes the duration of the k-th region; and $\tau_k(k = 1, 2, \ldots, 7)$ denotes the relative time that starts at the beginning of the k-th region.

In the real machining segment, the S-curve profile may not include the whole seven regions shown in Fig. 1. According to the starting velocity v_s, the ending velocity v_e, the instruction feedrate F, the machining segment length l, the interpolation period T, the maximum allowable acceleration $a_{\max}$, and the maximum allowable jerk $j_{\max}$, one or more regions may not be included in the S-curve profile. In the following paragraphs, the discrete S-curve speed control algorithm is derived. The procedure of the algorithm consists of the displacements of acceleration process and deceleration process pre-computation, the actual maximum feedrate computation, the ACC/DEC type judgment and the deceleration point forecast, and the feedrate computation in each interpolation period.

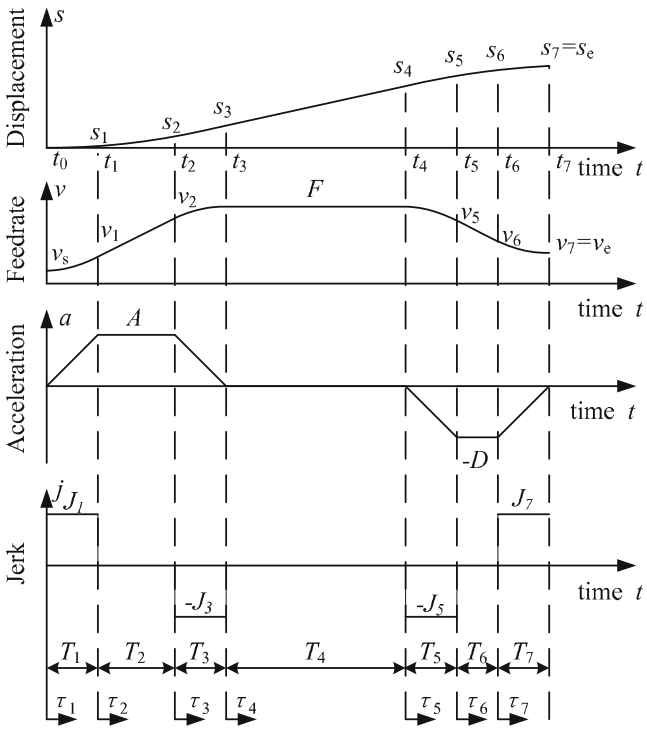

Fig. 1 Kinematic profiles of S-curve ACC/DEC process

2.1 The displacements of acceleration process and deceleration process pre-computation

In this section, in order to express and compute conveniently, the uniform formulas of the displacements for both acceleration process and deceleration process are derived.

Suppose the starting and the ending velocity of the acceleration (deceleration) process are V_1 and V_2, respectively. Let $N_{\mathrm{m}} = \lfloor a_{\max}/(j_{\max}T) \rfloor$, where $\lfloor \cdot \rfloor$ denotes the floor integer. To simplify calculation, assume that the displacement of feedrate varied from V_1 to V_2 equals to the displacement of feedrate varied from V_2 to V_1. To guarantee this property, the duration of accelerated acceleration (deceleration) region is two interpolation periods longer than the duration of decelerated acceleration (deceleration) region. According to where there is the constant acceleration (deceleration) region and where the achieved maximum acceleration magnitude $A_{\max}$ is integer times of $j_{\max}T$ or not, the acceleration profile can be divided into four types. Take acceleration process as an example, the four types of the acceleration profile are shown in Fig. 2. If $|V_1 - V_2| > N_{\mathrm{m}}^2 j_{\max} T^2$ holds, the constant acceleration region exists, as shown in Fig. 2a, c; otherwise, the constant acceleration region does not exist, as shown in Fig. 2b, d. If $|V_1 - V_2| = n_1(n_1 + n_2) j_{\max} T^2$ holds, where n_1 is one less than the number of interpolation periods of the accelerated acceleration region and n_2 denotes the number of interpolation periods of the constant acceleration region, then the achieved maximum acceleration magnitude $A_{\max}$ is integer times of $j_{\max}T$, as shown in Fig. 2a, b; otherwise, $A_{\max}$ is not integer times of $j_{\max}T$, as shown in Fig. 2c, d.

Considering the four different types of the acceleration profile of the acceleration (deceleration) process where the feedrate varies from V_1 to V_2, the uniform formulas of the acceleration a_j and the feedrate v_j in the j-th interpolation period and the theoretical

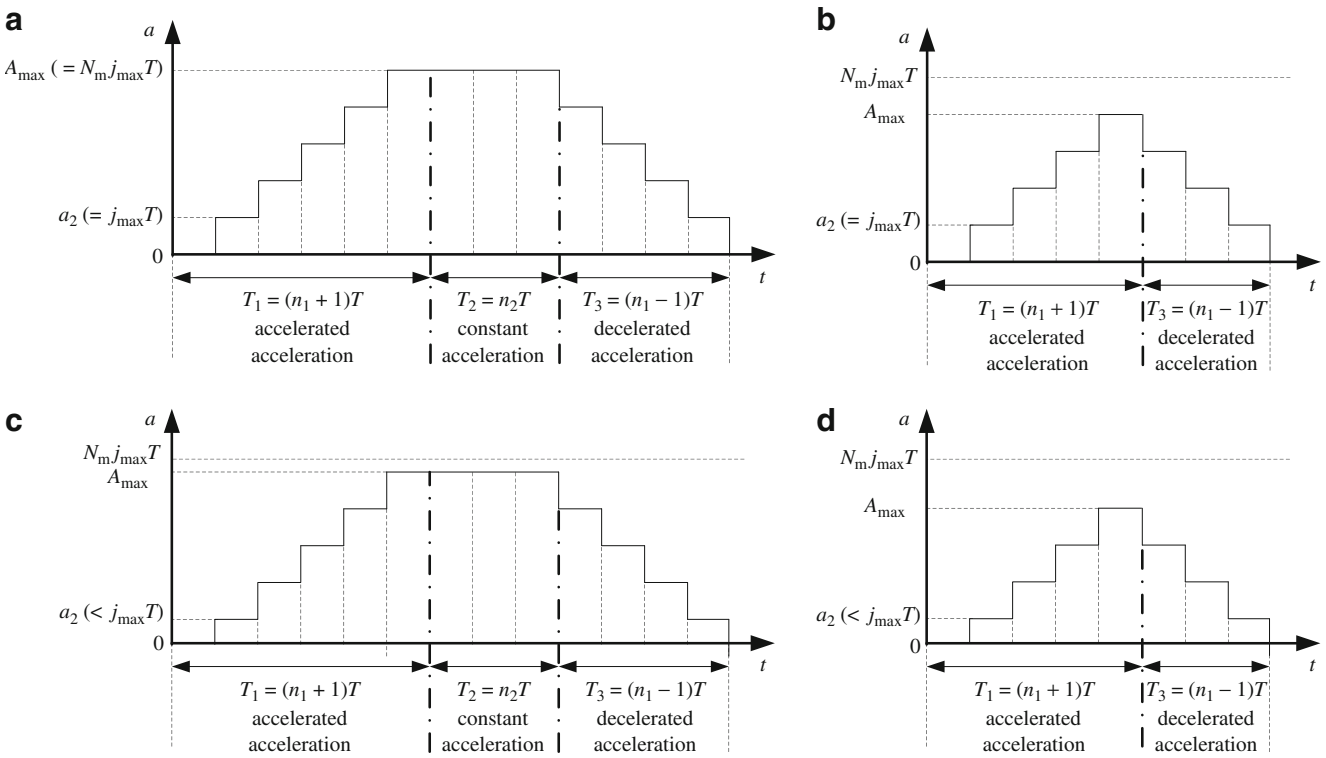

Fig. 2 Four types of the acceleration profile of acceleration process

displacement of the acceleration (deceleration) process $L_{th}(V_1, V_2, N_m)$ are written as

$$a_j = \begin{cases} 0 & j=1 \\ \hat{a}_2+(j-2)\hat{J}T & 1<j\le n_1+1 \\ \hat{a}_2+(n_1-1)\hat{J}T & n_1+1<j\le n_1+n_2+1 \\ \hat{a}_2+(2n_1+n_2-j)\hat{J}T & n_1+n_2+1<j\le 2n_1+n_2 \end{cases}, \tag{1}$$

$$v_j = \begin{cases} V_1 & j=1 \\ v_{j-1}+a_j T & 1<j\le 2n_1+n_2 \end{cases}, \tag{2}$$

$$\begin{aligned} L_{th}(V_1, V_2, N_m) &= \sum_{i=1}^{2n_1+n_2} v_i T \\ &= (2n_1+n_2)V_1 T + \frac{1}{2}\hat{a}_2(4n_1^2+4n_1n_2 \\ &\quad +n_2^2-2n_1-n_2)T^2+\frac{1}{2}(2n_1^3+3n_1^2n_2 \\ &\quad +n_1n_2^2-4n_1^2-4n_1n_2-n_2^2+2n_1 \\ &\quad +n_2)\hat{J}T^3. \end{aligned} \tag{3}$$

In Eqs. 1, 2, and 3, the parameters n_1, n_2, $\hat{a}_2$, and $\hat{J}$ are defined as

$$n_1 = \begin{cases} N_m & M_1 > 0 \\ \lceil M_2 \rceil & M_1 \le 0 \end{cases}, \; n_2 = \begin{cases} \lceil M_1 \rceil & M_1 > 0 \\ 0 & M_1 \le 0 \end{cases},$$

$$\hat{a}_2 = \begin{cases} A_2 & V1 < V2 \\ -A_2 & V1 > V2 \end{cases}, \; \hat{J} = \begin{cases} j_{max} & V1 < V2 \\ -j_{max} & V1 > V2 \end{cases},$$

where $M_1 = \frac{|V_1-V_2|}{N_m j_{max} T^2} - N_m$, $M_2 = \sqrt{\frac{|V_1-V_2|}{j_{max} T^2}}$, $\lceil \cdot \rceil$ denotes the ceiling-integer and $A_2 = \frac{1}{(2n_1+n_2-1)T} \times [|V_1-V_2| - (n_1-1)(n_1+n_2-1) j_{max} T^2]$.

According to Eq. 3, let $V_1 = v_s$ and $V_2 = F$, the displacement of the acceleration process is pre-computed as

$$L_1 = L_{th}(v_s, F, N_m), \tag{4}$$

and similarly, let $V_1 = F$ and $V_2 = v_e$, the displacement of the deceleration process is pre-computed as

$$L_2 = L_{th}(F, v_e, N_m). \tag{5}$$

2.2 The actual maximum feedrate computation

The actual maximum feedrate v_m is related to the machining segment length l. As shown in Fig. 3, there are two cases of the computation of v_m.

In the case of Fig. 3a, the length l is long enough to achieve the instruction feedrate F, namely $l \ge L_1 + L_2$, then $v_m = F$. In the case of Fig. 3b, the length l is too short to achieve the instruction feedrate F, and the type of ACC/DEC is acceleration–deceleration mode. As the displacement of the acceleration–deceleration

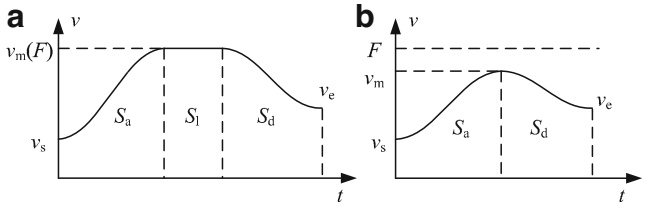

Fig. 3 Feedrate profiles of S-curve ACC/DEC. **a** With constant velocity region. **b** Without constant velocity region

process is the monotonic increasing function of the actual maximum feedrate v_m, v_m can be computed using dichotomy.

The pseudo-code of the actual maximum feedrate computation is given in Algorithm 1, where S_m^k denotes the displacement of the acceleration–deceleration process in the k-th iteration, and *maxErr* denotes the maximum allowable displacement error.

Algorithm 1: Computation of actual maximum feedrate

Input: v_s, v_e, F, l, N_m, L_1, L_2 and $maxErr$
Output: the actual maximum feedrate v_m
if $L_1 + L_2 \leq l$ **then**
  $v_m \leftarrow F$;
else
  $k \leftarrow 0$, $v_L^k \leftarrow \max\{v_s, v_e\}$ and $v_H^k \leftarrow F$;
  $v_m^k \leftarrow \frac{1}{2}(v_L^k + v_H^k)$;
  $S_m^k \leftarrow L_{th}(v_s, v_m^k, N_m) + L_{th}(v_m^k, v_e, N_m)$;
  while $|S_m^k - l| > maxErr$ **do**
    $k \leftarrow k + 1$;
    if $S_m^k < l$ **then**
      $v_L^k \leftarrow v_m^k$;
    else
      $v_H^k \leftarrow v_m^k$;
    $v_m^k \leftarrow \frac{1}{2}(v_L^k + v_H^k)$;
    $S_m^k \leftarrow L_{th}(v_s, v_m^k, N_m) + L_{th}(v_m^k, v_e, N_m)$;
  $v_m \leftarrow v_m^k$;
return v_m

2.3 Acceleration and deceleration type judgment and deceleration point forecast

The type of ACC/DEC can be judged by comparing v_m with v_s and v_e. If $v_s < v_m$, then the acceleration process exists; otherwise, it does not exist. If $v_e < v_m$, then the deceleration process exists; otherwise, it does not exist.

From Eq. 3, the length of deceleration region can be computed as

$$S_d = \min\{L_{th}(v_m, v_e, N_m), l\}. \tag{6}$$

And the rule to forecast the deceleration point is that, once the remaining length of the machining segment is not more than the length of deceleration region, the deceleration process gets started.

2.4 Feedrate computation in each interpolation period

If $v_s < v_m$, then the acceleration process exists. Let $V_1 = v_s$ and $V_2 = v_m$, then the law of feedrate variation in the acceleration process can be computed by using Eq. 2.

If the feedrate equals to v_m and the remaining length of the machining segment is more than the length of deceleration region, then the process is in the constant velocity region, and feedrate equals to v_m.

If $S_d > 0$ and the remaining length of the machining segment is not more than the length of deceleration region, then the deceleration process will start. Let $V_1 = v_m$ and $V_2 = v_e$, then the law of feedrate variation in the deceleration process can also be computed by using Eq. 2.

3 Look-ahead and adaptive speed control algorithm

In this section, a look-ahead and adaptive speed control algorithm based on the discrete S-curve ACC/DEC is presented. Linked feedrate constraints are derived under the condition of the axis feedrate and feed acceleration limits, the circular arc radius error limit, and the machining segment length limit. As the discrete S-curve ACC/DEC is adopted, it is hard to find the analytic expression for the optimal linked feedrate with these constraints. Thus, an iterative look-ahead and adaptive algorithm is presented to seek the optimal linked feedrate in the scope of the maximum preprocessing segments. Because the actual ending velocity of machining segment equals to the corresponding optimal linked feedrate, the ACC/DEC control of current segment can be executed easily according to the ACC/DEC control algorithm described in Section 2.

3.1 Linked feedrate constraints of S-curve ACC/DEC

Suppose $v_{s,h}$, $v_{e,h}$, F_h, l_h, and $a_{\max,h} = N_{m,h} j_{\max} T$ are the starting velocity, the ending velocity, the instruction feedrate, the machining segment length, and the maximum allowable acceleration of the h-th segment $l(h)$, respectively. To realize smooth connection of the feedrate at the transition point, the ending velocity of segment $l(h)$ should equal to the starting velocity of segment $l(h+1)$, namely $v_{e,h} = v_{s,h+1}$. In the following paragraphs, the constraints of linked feedrate $v_{e,h}$ between segments $l(h)$ and $l(h+1)$ using S-curve ACC/DEC algorithm are derived under the condition of the axis feedrate and feed acceleration limits, the circular arc radius error limit, and the machining segment length limit.

3.1.1 The axis feedrate and feed acceleration limits

Suppose the maximum feedrate and maximum feed acceleration of axis Λ are $v_{\Lambda\max}$ and $a_{\Lambda\max}$, respectively, where $\Lambda = x, y, z$. With the axis feedrate limits, the linked feedrate $v_{e,h}$ satisfies:

$$\begin{cases} v_{e,h} \cdot |e_{\Lambda e,h}| \le v_{\Lambda\max} \\ v_{e,h} \cdot |e_{\Lambda s,h+1}| \le v_{\Lambda\max} \end{cases}, \quad \Lambda = x, y, z, \tag{7}$$

where $(e_{xe,h}, e_{ye,h}, e_{ze,h})'$ and $(e_{xs,h+1}, e_{ys,h+1}, e_{zs,h+1})'$ denote the unit direction vector at the ending point of segment $l(h)$ and at the starting point of segment $l(h+1)$, respectively.

Thus, $v_{e,h}$ satisfies the following inequality

$$v_{e,h} \le v^{(1)}_{e\max,h} = \min_{\Lambda=x,y,z} \left\{ \frac{v_{\Lambda\max}}{|e_{\Lambda e,h}|}, \frac{v_{\Lambda\max}}{|e_{\Lambda s,h+1}|} \right\}. \tag{8}$$

With the axis feed acceleration limits [7], $v_{e,h}$ satisfies:

$$|v_{e,h} \cdot e_{\Lambda s,h+1} - v_{e,h} \cdot e_{\Lambda e,h}| \le a_{\Lambda\max} T, \quad \Lambda = x, y, z, \tag{9}$$

From Eq. 9, $v_{e,h}$ satisfies the following formula

$$v_{e,h} \le v^{(2)}_{e\max,h} = \min_{\Lambda=x,y,z} \left\{ \frac{a_{\Lambda\max} T}{|e_{\Lambda s,h+1} - e_{\Lambda e,h}|} \right\}. \tag{10}$$

3.1.2 The circular arc radius error limit

If segment $l(h)$ and/or segment $l(h+1)$ are circular arc paths, the linked feedrate $v_{e,h}$ should satisfy the circular arc radius error limit [14] as shown in Fig. 4. Suppose the circular arc radius is R, the feedrate is v and the step angle is γ, then the maximum radius error can be written as

$$e_R = R\left(1 - \cos\frac{\gamma}{2}\right) \approx R\left(1 - \cos\frac{vT}{2R}\right) \approx \frac{v^2 T^2}{8R}. \tag{11}$$

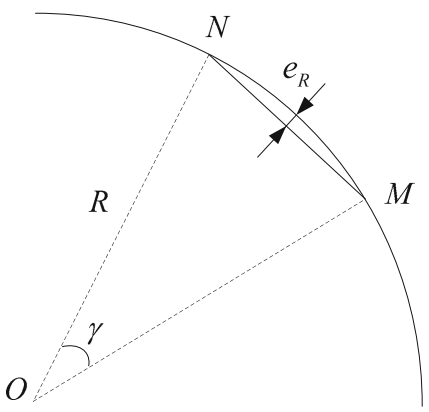

Fig. 4 Radius error of circular arc interpolation

From Eq. 11, the following inequality of the feedrate $v_{e,h}$ should be satisfied

$$v_i \le v^{(arc)}_{\max} = \sqrt{8Re_R}/T. \tag{12}$$

According to Eqs. 8, 10, and 12, $v_{e,h}$ satisfies

$$v_{e,h} \le v_{e\max,h} = \min\left\{ v^{(1)}_{e\max,h}, v^{(2)}_{e\max,h}, v^{(arc)}_{\max} \right\}, \tag{13}$$

where $v_{e\max,h}$ is the upper limit of the linked feedrate between the machining segments $l(h)$ and $l(h+1)$.

3.1.3 The machining segment length limit

The linked feedrate $v_{e,h}$ is also limited by the machining segment length. Suppose that throughout the segment $l(h)$, the feedrate accelerates from $v_{e,h-1}$ to $v_{e,h}$ using S-curve ACC/DEC algorithm. And $v_{e,h}$ may be less than the instruction feedrate F_h because of the segment length limit. The relation formula of $v_{e,h-1}$ and $v_{e,h}$ is given by

$$v_{e,h} \le V_{th}(l_h, v_{e,h-1}, F_h, N_{m,h}), \tag{14}$$

where the function $V_{th}(l, v_s, v_{\text{obj}}, N_m)$ is used for computing the actual ending velocity of the S-curve acceleration (deceleration) process when the segment length is l, the starting velocity is v_s, the target velocity is v_{obj}, and the maximum allowable acceleration is $N_m j_{\max} T$. The computation of $V_{th}(l, v_s, v_{\text{obj}}, N_m)$ is given in Algorithm 2, where S^k_{th} denotes the theoretical displacement of the acceleration (deceleration) process in the k-th iteration.

Algorithm 2: Computation of function $V_{th}(l, v_s, v_{obj}, N_m)$

Input: v_s, v_{obj}, l, N_m and $maxErr$
Output: the function value $v_{th} = V_{th}(l, v_s, v_{obj}, N_m)$
if $v_s = v_{obj}$ *or* $l \ge L_{th}(v_s, v_{obj}, N_m)$ **then**
  $v_{th} \leftarrow v_{obj}$;
else
  $k \leftarrow 0$, $v^k_L \leftarrow \min\{v_s, v_{obj}\}$ and $v^k_H \leftarrow \max\{v_s, v_{obj}\}$;
  $v^k_{th} \leftarrow \frac{1}{2}(v^k_L + v^k_H)$;
  $S^k_{th} \leftarrow L_{th}(v_s, v^k_{th}, N_m)$;
  while $|S^k_{th} - l| > maxErr$ **do**
    $k \leftarrow k + 1$;
    if $(v_s - v_{obj}) \cdot (S^k_{th} - l) > 0$ **then**
      $v^k_L \leftarrow v^k_{th}$;
    else
      $v^k_H \leftarrow v^k_{th}$;
    $v^k_{th} \leftarrow \frac{1}{2}(v^k_L + v^k_H)$;
    $S^k_{th} \leftarrow L_{th}(v_s, v^k_{th}, N_m)$;
  $v_{th} \leftarrow v^k_{th}$;
return v_{th}

Similarly, suppose that throughout the segment $l(h+1)$, the feedrate decelerates from $v_{e,h}$ to $v_{e,h+1}$ using

S-curve ACC/DEC algorithm, and the relation formula of $v_{e,h}$ and $v_{e,h+1}$ is given by

$$v_{e,h} \le V_{th}(l_{h+1}, v_{e,h+1}, F_{h+1}, N_{m,h+1}). \tag{15}$$

Suppose the number of the segments of the tool path is N. Obviously, the starting velocity of the first machining segment $l(1)$ and the ending velocity of the last machining segment $l(N)$ are zero, namely $v_{e,0} = 0$ and $v_{e,N} = 0$. And from Eqs. 13, 14, and 15, the constraints of the linked feedrate $v_{e,h}$ can be formulated as

$$\begin{cases} v_{e,h} \le v_{e\max,h}, & h = 0, 1, \cdots, N \\ v_{e,h} \le V_{th}(l_h, v_{e,h-1}, F_h, N_{m,h}), & h = 1, 2, \cdots, N \\ v_{e,h} \le V_{th}(l_{h+1}, v_{e,h+1}, F_{h+1}, N_{m,h+1}), & h = 0, 1, \cdots, N-1 \\ v_{e,0} = 0 \\ v_{e,N} = 0 \end{cases} \tag{16}$$

3.2 The optimal linked feedrate pre-computation

Suppose the optimal linked feedrate between segments $l(h)$ and $l(h+1)$ is $v^*_{e,h}$. In order to gain maximum productivity, the optimal linked feedrate sequence $(v^*_{e,0}, v^*_{e,1}, \cdots, v^*_{e,N})$ of the tool path is sought to maximize $(v_{e,0}, v_{e,1}, \cdots, v_{e,N})'$ with constraints Eq. 16 as

$$(v^*_{e,0}, v^*_{e,1}, \cdots, v^*_{e,N}) = \underset{v_{e,h}, \forall h \in [0,N]}{\arg\max} \ (v_{e,0}, v_{e,1}, \cdots, v_{e,N})', \quad \textit{subject to Eq. 16.} \tag{17}$$

From Eq. 16, the linked feedrate $v_{e,h}$ is limited not only by the upper limit of the linked feedrate $v_{e\max,h}$ but also by $v_{e,h-1}$ and l_h and by $v_{e,h+1}$ and l_{h+1}. According to the definition of the optimal linked feedrate, $v_{e,h-1} \le v^*_{e,h-1}$ holds. Because the function $v_{th} = V_{th}(l, v_s, v_{\text{obj}}, N_m)$ described in Algorithm 2 is a monotonic increasing function of the starting velocity v_s, then

$$V_{th}(l_h, v_{e,h-1}, F_h, N_{m,h}) \le V_{th}(l_h, v^*_{e,h-1}, F_h, N_{m,h}). \tag{18}$$

Thus, the optimization problem 17 can be rewritten as

$$\begin{aligned} v^*_{e,h} = \underset{v_{e,h}}{\arg\max} \ & v_{e,h}, \quad h = 1, 2, \cdots, N \\ \textit{subject to} \ & v_{e,j} \le v_{e\max,j}, \quad j = h, h+1, \cdots, N \\ & v_{e,h} \le V_{th}(l_h, v^*_{e,h-1}, F_h, N_{m,h}) \\ & v_{e,j} \le V_{th}(l_{j+1}, v_{e,j+1}, F_{j+1}, N_{m,j+1}), \\ & \qquad j = h, h+1, \cdots, N-1 \\ & v^*_{e,0} = v_{e,0} = 0 \\ & v_{e,N} = 0 \end{aligned} \tag{19}$$

From problem 19, the feedrate $v_{e,h}$ is limited by $v_{e\max,h}$, $V_{th}(l_h, v^*_{e,h-1}, F_h, N_{m,h})$ and the latter machining segments. And the limitation of $v_{e,h}$ by the latter machining segments can be sought by an iterative calculation whose recurrence relation is as follows:

$$\begin{aligned} v^{(1)}_{e,j} = \min\{ & V_{th}(l_{j+1}, v^{(1)}_{e,j+1}, F_{j+1}, N_{m,j+1}), v_{e\max,j}\}, \\ & j = N-1, N-2, \cdots, h, \end{aligned} \tag{20}$$

where $v^{(1)}_{e,j}$ whose initial value is $v^{(1)}_{e,N} = v_{e,N} = 0$ denotes the corrected ending velocity of segment $l(j)$.

Therefore, $v^*_{e,h}$ is computed as

$$v^*_{e,h} = \min\{V_{th}(l_h, v^*_{e,h-1}, F_h, N_{m,h}), v^{(1)}_{e,h}\}. \tag{21}$$

According to Eq. 20, it would need calculation for at most $(N-h)$ times to solve $v^{(1)}_{e,h}$, which would be very slow and inefficient in the case of a large N. In order to improve the calculation efficiency, the maximum number of look-ahead segments N_t is preset, and the maximum times of the iterative calculation would not exceed it. In the following paragraph, the optimal linked feedrate is sought in the scope of the maximum preprocessing segments. Suppose the labels of the preprocessing segments are $h = i, i+1, \cdots, i+N_t-1$, the optimal linked feedrate $v^*_{e,i-1}$ between segments $l(i-1)$ and $l(i)$ is known, and $v_{s,i} = v^*_{e,i-1}$ holds. The procedure of the pre-computation of the optimal linked feedrate $v^*_{e,i}$ using the look-ahead method is given in Algorithm 3, where $v^{(0)}_{e,i}$ denotes the ending velocity of segment $l(i)$ by the means of S-curve acceleration, and $v^{(1)}_{e,i+K}$

denotes the backward corrected ending velocity of segment $l(i+K)$ by the means of S-curve acceleration.

Algorithm 3: Pre-computation of the optimal linked feedrate

Input: $v^*_{e,i-1}$, l_h, F_h, $N_{m,h}$ and $v_{e\max,h}$, where $h = i, i+1, \cdots, i+N_t-1$
Output: the optimal linked feedrate $v^*_{e,i}$ between segments $l(i)$ and $l(i+1)$

```
n ← 0;
while v_{e max,i+n} > 0 and n < N − t − 1 and segment
l(i + n + 1) is motion control instruction do
    n ← n + 1;
if n = 0 then
    v*_{e,i} ← 0;
else
    v^(0)_{e,i} ← V_th(l_i, v*_{e,i−1}, F_i, N_{m,i});
    K ← n and v^(1)_{e,i+K} ← 0;
    while K ≥ 1 do
        v^(1)_{e,i+K} ← V_th(l_{i+K}, v^(1)_{e,i+K}, F_{i+K}, N_{m,i+K});
        v^(1)_{e,i+K} ← min{v^(1)_{e,i+K}, v_{e max,i+K−1}};
        K ← K − 1;
    v*_{e,i} ← min{v^(0)_{e,i}, v^(1)_{e,i+K}};
return v*_{e,i}
```

3.3 Adaptive S-curve speed control of current segment

The actual ending velocity of the current segment $l(i)$ equals the corresponding optimal linked feedrate $v^*_{e,i}$, which is computed as Algorithm 3 in Section 3.2. Then the adaptive S-curve ACC/DEC control algorithm of the current segment $l(i)$ is given in the following paragraph, based on its instruction feedrate F_i, actual starting velocity $v^*_{e,i-1}$, actual ending velocity $v^*_{e,i}$, segment length l_i, and maximum allowable acceleration $a_{\max,i} = N_{m,i} j_{\max} T$.

Let $F = F_i$, $v_s = v^*_{e,i-1}$, $v_e = v^*_{e,i}$, $l = l_i$, and $a_{\max} = a_{\max,i}$, the adaptive S-curve ACC/DEC control algorithm of the current segment $l(i)$ can be executed according to the discrete S-curve speed control algorithm described in Section 2. And the procedure of the algorithm consists of the displacements of acceleration process and deceleration process pre-computation, the practical maximum feedrate computation, the ACC/DEC type judgment and the deceleration point forecast, and the feedrate computation in each interpolation period.

According to the look-ahead and adaptive speed control algorithm described in Section 3, the flowchart of the proposed algorithm is given in Fig. 5, where n_r denotes the number of the machining segments without the optimal linked feedrate pre-computation and v_j denotes the feedrate of the current segment $l(i)$ in the j-th interpolation period.

4 The implementation of the proposed speed control algorithm

Typical foreground and background frame is adopted in the implementation of the proposed speed control algorithm for high-speed CNC systems as shown in Fig. 6. The foreground program, mainly for adaptive S-curve ACC/DEC speed control and the interpolation calculation of current machining segment $l(i)$, is realized by using timer interrupt service routine to compute the displacement increment of each axis in each interpolation period. And the background program, whose main functions are numerical control (NC) code compiler, cutter compensation, optimal feedrate pre-computation using the look-ahead method, is to prepare multiple NC segments for machining in the future.

To effectively prevent the data hunger caused by high feedrate and short machining segment length, multiple segments feedrate planning, where M subsequent machining segments are prepared, is adopted in the background program. As shown in Fig. 6a, there are three kinds of buffers: AS buffer, BS buffer, and CS buffer. AS buffer is used for storing the motion control instruction of the current segment $l(i)$. According to its content, the adaptive S-curve ACC/DEC speed control and the interpolation calculation of the current segment $l(i)$ are executed. BS buffer, which is made up of $N_t + M$ buffer registers, is used for preparing M subsequent machining segments of segment $l(i+1)$ to segment $l(i+M)$ with the optimal linked feedrate pre-computation. The latter N_t buffer registers of BS buffer, BSReg$[M+1]$ to BSReg$[M+N_t]$, are used for storing the machining segments $l(i+M+1)$ to $l(i+M+N_t)$ without the optimal linked feedrate pre-computation, respectively. And the former M buffer registers, BSReg[1] to BSReg$[M]$, are used for storing the machining segments $l(i+1)$ to $l(i+M)$ with the optimal linked feedrate pre-computation, respectively. And CS buffer is used for loading new segment of NC code.

Let ASFlag be the status flag of AS buffer, where ASFlag=1 means AS buffer is not empty, namely the interpolation of current machining segment $l(i)$ is not completed and ASFlag=0 means AS buffer is empty. And let PreFlag be the ACC/DEC pre-computation status flag of current segment $l(i)$, where PreFlag=1 means the ACC/DEC pre-computation of segment $l(i)$ is executed, and PreFlag=0 means the ACC/DEC pre-computation has not been executed. The data flow of these buffers is as follows: When ASFlag=0 and BSReg[1] is not empty, the content of BSReg[1] is stored in AS buffer, and ASFlag and

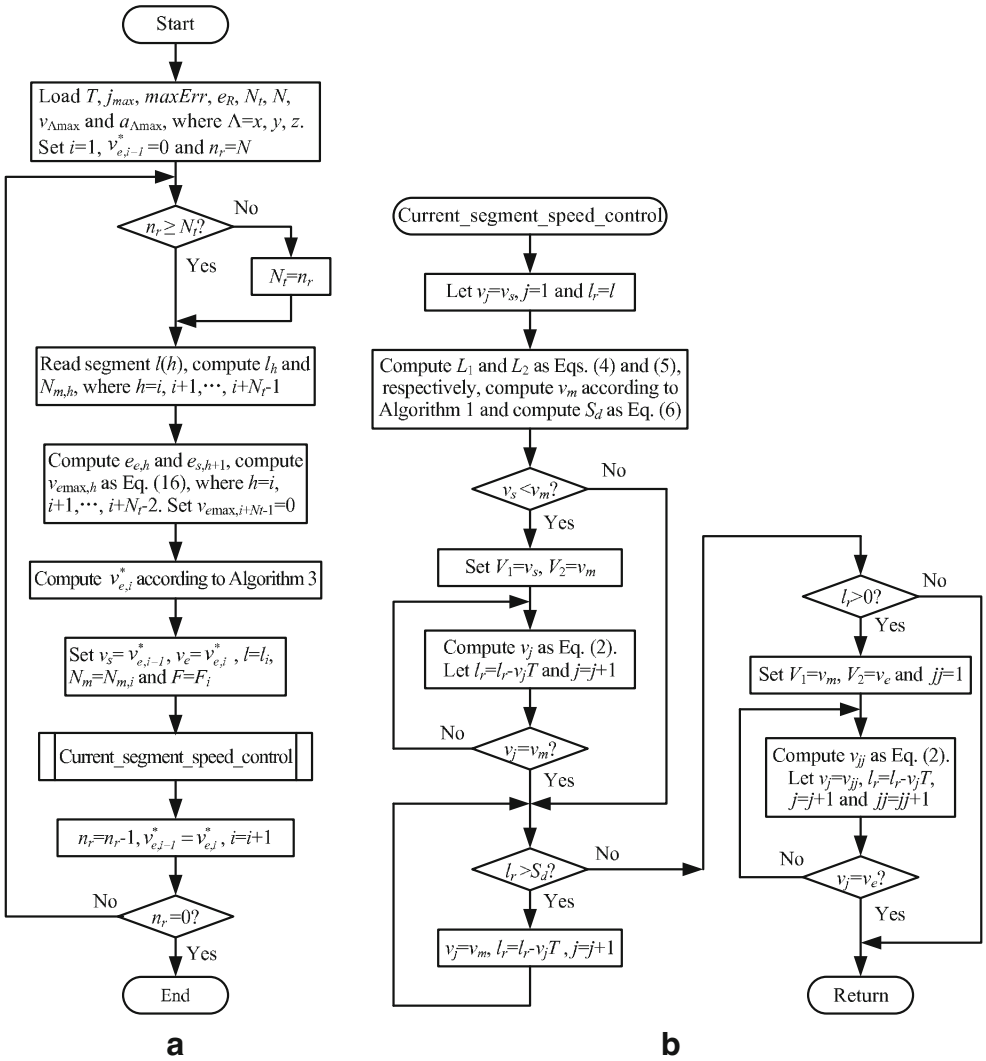

Fig. 5 Flowchart of the proposed look-ahead and adaptive speed control algorithm. **a** Main program. **b** Subroutine of the current segment speed control

PreFlag are set to 1 and 0, respectively. Then the content of BSReg$[p+1]$ is shifted to BSReg$[p]$, where $p = 1, 2, \cdots, M-1$. When the buffer register BSReg$[M]$ is empty and BSReg$[M+1]$ is not empty, according to the contents of the latter N_t buffer registers of BSReg$[M+1]$ to BSReg$[M+N_t]$, the optimal linked feedrate $v^*_{e,i+M+1}$ between segments $l(i+M+1)$ and $l(i+M+2)$ is computed using the look-ahead method given in Algorithm 3. Then the content of BSReg$[M+1]$ and $v^*_{e,i+M+1}$ are stored in BSReg$[M]$, the content of BSReg$[M+q+1]$ is shifted to BSReg$[M+q]$, where $q = 1, 2, \cdots, N_t-1$, and the content of CS buffer is stored in BSReg$[M+N_t]$. When CS buffer is empty and there exists NC code without processing, new segment is loaded to store in CS buffer.

In the foreground program as shown in Fig. 6b, when ASFlag is 1, the adaptive S-curve ACC/DEC speed control and interpolation calculation of current segment $l(i)$ are executed. If PreFlag is 0, which means a new motion control instruction has just been read from AS buffer, then the pre-computation of S-curve ACC/DEC is executed, including the displacement of the acceleration process and deceleration process, respectively, computed as Eqs. 4 and 5, the actual maximum feedrate computed as Algorithm 1 and the length of deceleration region computed as Eq. 6. Meanwhile, PreFlag and the current number of interpolation period are both set to 1. Otherwise, the feedrate v_j in the j-th interpolation period is computed according to the law of discrete S-curve ACC/DEC speed control

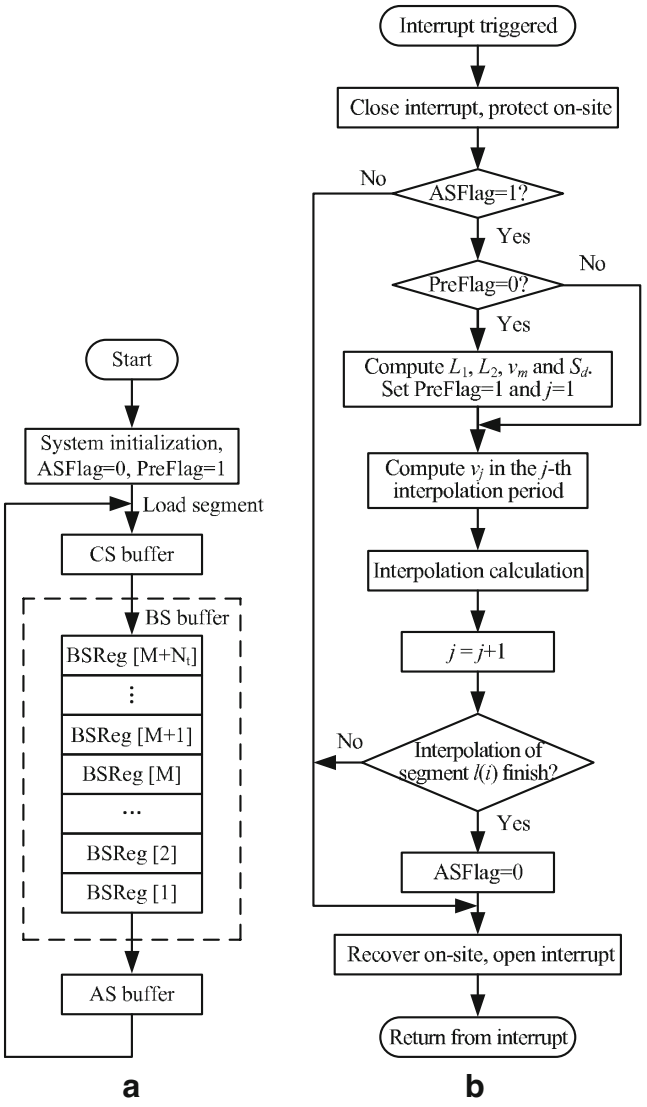

Fig. 6 The implementation of the look-ahead and adaptive speed control algorithm for high-speed CNC systems. **a** The flowchart of background program. **b** The flowchart of foreground program

as described in Section 3.3 and Fig. 5b. Then v_j is transferred to the interpolation calculation module to compute the displacement increment of each axis in each interpolation period. Once the interpolation of current segment $l(i)$ is completed, ASFlag is set to 0.

5 Experimental results

5.1 Simulation experiments

In the simulation, the parameters are defined as follows: the interpolation period $T = 4$ ms, the maximum feedrate of axis x is 15 m/min, the maximum feedrate of both axis y and axis z is 12 m/min, the maximum feed acceleration of each axis is 5 m/s^2, the maximum allowable jerk $j_{\max}$ is 50 m/s^3, the maximum allowable displacement error $maxErr$ is 0.01 mm, and the maximum radius error e_R is 5 μm.

The validity of the proposed algorithm is demonstrated with different values of maximum number of look-ahead segments N_t. The simulated tool path of ten line blocks is shown in Fig. 7, and the instruction feedrate is 6 m/min. The comparison of feedrate profiles with three different N_t of 1, 2, and 3 is shown in Fig. 8. As shown in Fig. 8, there are no feedrate gusts with different N_t, and the feedrates are smooth. When the maximum number of look-ahead segments $N_t = 1$, the starting and ending velocities of each segment are forced to zero, which is known as the traditional control method. The machining time of $N_t = 2$ and 3 is 464 and 432 ms, respectively, whereas the machining time of $N_t = 1$ is 1,184 ms. Thus, the proposed algorithm reduces the machining time significantly and greatly improves the productivity. The relationship between the machining time and the maximum number of look-ahead segments is shown in Fig. 9. From Fig. 9, the machining time gradually decreases with increasing N_t from 1 to 5, and it becomes constant with $N_t \geq 5$. Because more calculation time of seeking the optimal linked feedrate is needed and there is no decrease in the machining time, it is not necessary to choose a very large N_t. With the requirement of real-time computation, the proper N_t should be chosen to improve the machining efficiency.

In the following paragraphs, the influence factors of choosing the proper maximum number of look-ahead segments N_t are discussed, including the machining segment length and the instruction feedrate. Suppose a tool path composed of m equal-length straight-line segments is a straight line, whose starting and ending points are $(0, 0, 0)$ and $(500, 0, 0)$ mm, respectively. As the whole length of the tool path is 500 mm, the

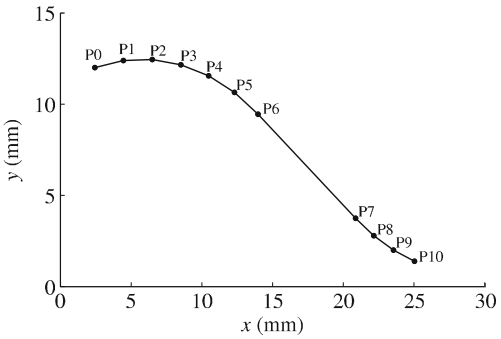

Fig. 7 The simulated tool path

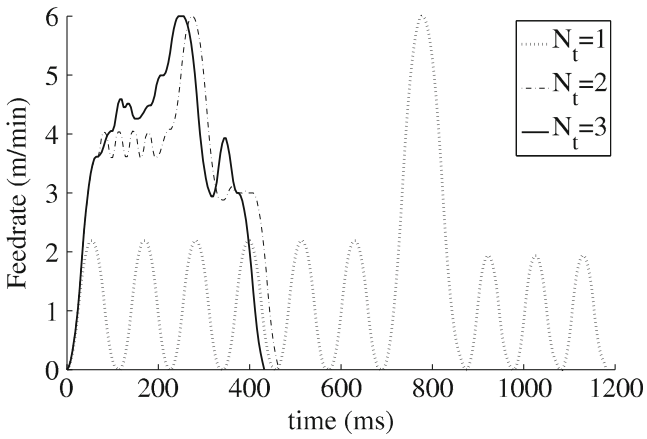

Fig. 8 Comparison of feedrate profiles with different maximum number of look-ahead segments

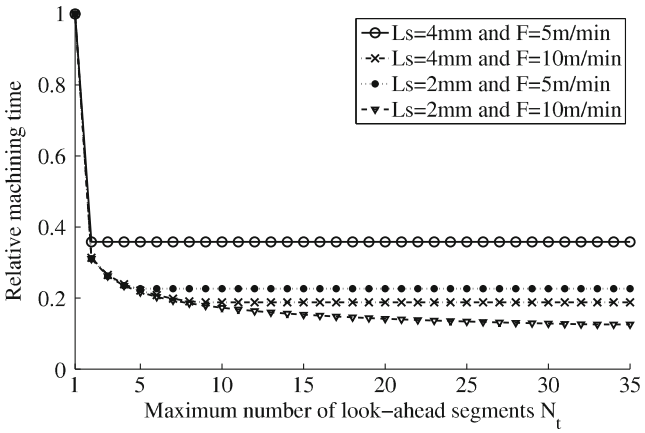

Fig. 10 The relative machining time vs. the maximum number of look-ahead segments with different machining segment lengths and instruction feedrates

machining segment length of each segment $L_s = 500/m$ mm. That is, the endpoints of the tool path are $(0, 0, 0)$ mm, $(L_s, 0, 0)$ mm, $(2L_s, 0, 0)$ mm, $\cdots$, $(mL_s, 0, 0)$ mm.

The machining segment length L_s are, respectively, set to 2 and 4 mm, and the instruction feedrates F are, respectively, set to 5 and 10 m/min. The relationship between the relative machining time and the maximum number of look-ahead segments N_t with different machining segment lengths and instruction feedrate is shown in Fig. 10. And the relative machining time of $N_t = k$ is defined as the machining time of $N_t = k$ divided by the machining time of $N_t = 1$. As shown in Fig. 10, when the machining segment length $L_s = 4$ mm and the instruction feedrate $F = 5$ m/min, the minimum relative machining time is 0.3581 with $N_t \geq 2$, and the proper N_t should be 2; when $L_s = 4$ mm and $F = 10$ m/min, the minimum relative machining time is 0.1880 with $N_t \geq 9$, and the proper N_t should be 9; when $L_s = 2$ mm and $F = 5$ m/min, the minimum relative machining time is 0.2265 with $N_t \geq 5$, and the proper N_t should be 5; when $L_s = 2$ mm and $F = 10$ m/min, the minimum relative machining time is 0.1256 with $N_t \geq 33$, and the proper N_t should be 33. Therefore, the proper N_t should increase with decreasing of the segment length and increasing of the instruction feedrate.

When $L_s = 4$ mm and $F = 10$ m/min, the comparison of the feedrate profiles of the m equal-length straight-line tool path with different N_t is shown in Fig. 11. From Fig. 11a, the feedrate of $N_t = 1$ involves frequent acceleration and deceleration, and the machining time and the actual maximum feedrate are 17,000 ms and 3.345 m/min, respectively. Thus, the average feedrate of the tool path is 1.765 m/min, which is much lower than the instruction feedrate of 10 m/min. From Fig. 11b, the machining time and the actual maximum feedrate of $N_t = 10$ are 3, 196 ms and 10.005 m/min, respectively, and the average feedrate of the tool path is 9.387 m/min, which is about 5.3 times of the one of $N_t = 1$. Therefore, the proposed look-ahead and adaptive speed control algorithm can effectively reduce the machining time and avoid frequent acceleration and deceleration.

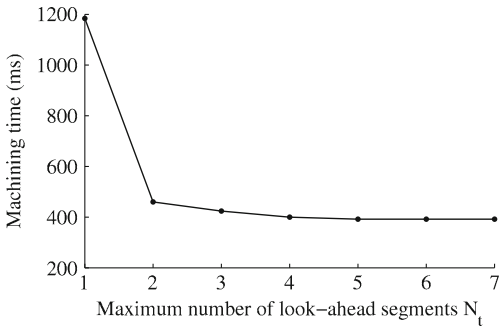

Fig. 9 The machining time vs. the maximum number of look-ahead segments

5.2 Real experiments

The six-axis pipe cutting CNC system, which adopts the proposed speed control algorithm, has been applied to a six-axis pipe cutting robot. LGK160I inverter air plasma cutting machine is adopted in the pipe cutting robot for pipe cutting. And the processer adopted in the CNC system is TI TMS320F2812 DSP.

The cutting precision of the pipe cutting robot adopting the proposed speed control algorithm is experimented. In the real machining environment, the designed maximum cutting precision is required to be 1 mm. The parameters are defined as follows: $T = 4$ ms,

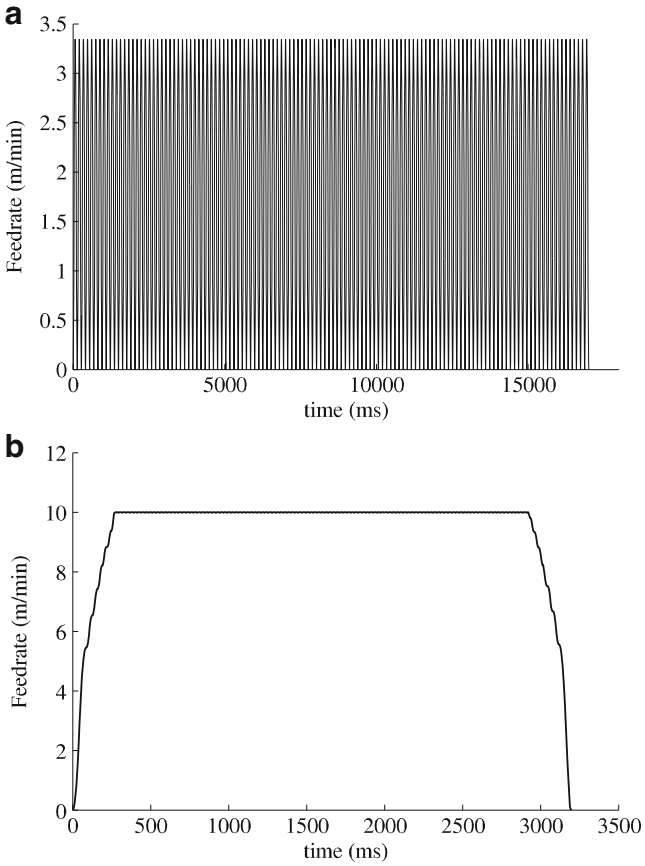

Fig. 11 Comparison of feedrate profiles of the m equal-length straight-line tool path with different N_t. **a** $N_t = 1$. **b** $N_t = 10$

the maximum feedrate of each axis is 12 m/min, the maximum feed acceleration of each axis is 5 m/s^2, $j_{\max} = 50$ m/s^3, $maxErr = 0.01$ mm, $e_R = 5$ μm, and the maximum number of look-ahead segments $N_t = 10$.

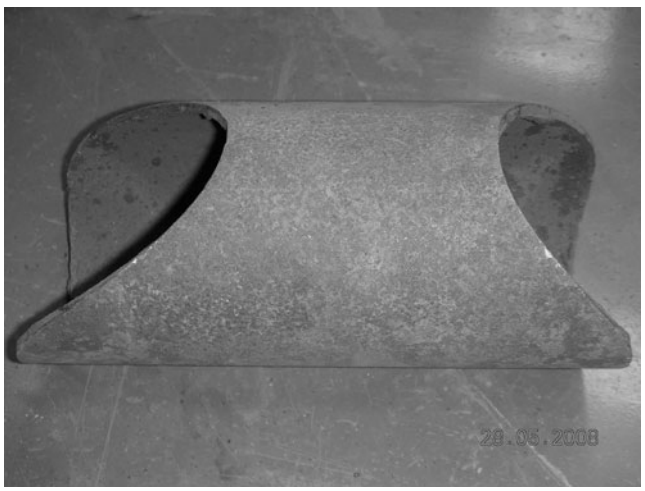

Fig. 12 The machined part of the branch pipe with dual ends

Actual cutting of various pipe ends is experimented, such as orthogonal end, skew end, skew truncated end, excentral skew end, dual intersectant end, dual skew truncated end, and branch pipe with dual ends, etc. And the results show that the cutting precision of 0.2 mm is attained, which satisfies the cutting precision requirement. The machined part of the branch pipe with dual ends is shown in Fig. 12. From Fig. 12, the cutting surface is very smooth.

Moreover, the calculation time of the proposed algorithm is tested in the pipe cutting CNC system. In the background program as shown in Fig. 6a, the calculation time of seeking the optimal linked feedrate is not more than 2.2 ms. And in the foreground program as shown in Fig. 6b, the feedrate in each interpolation period is computed using the adaptive S-curve ACC/DEC speed control algorithm described in Section 3.3, and its calculation time is not more than 1.2 ms. Therefore, the proposed algorithm can meet the real-time requirements for high-speed CNC machining.

6 Conclusions

To satisfy the requirements for high-speed machining, a novel look-ahead and adaptive speed control algorithm is presented in this paper. The algorithm is based on pre-interpolation S-curve ACC/DEC. Aiming at achieving the maximum feedrate in machining process, the optimal linked feedrate is sought in the scope of the maximum preprocessing segments by using the look-ahead method. With the optimal linked feedrate as the actual ending velocity of the corresponding machining segment, the ACC/DEC control of the segment is executed. The proposed algorithm has been applied to a pipe cutting CNC system to verify its effectiveness. The experimental results demonstrate that the proposed algorithm is a flexible speed control algorithm, which can overcome the drawbacks of traditional speed control method, realize high-speed, smooth linking of the feedrate, and avoid the acceleration gust.

References

1. Bedi S, Ali I, Quan N (1993) Advanced interpolation techniques for CNC machines. ASME J Eng Ind 115:329–336
2. Cao YN, Wang TM, Chen YD, Wei HX, Shao ZL (2008) A high-speed control algorithm using look-ahead strategy in

CNC systems. In: ICIEA 2008 Proceedings of 3rd IEEE Conference on Industrial Electronics and Applications, pp 372–377
3. Cui J, Chu ZY (2005) An improved approach for the acceleration and deceleration of industrial robots and CNC machine tools. In: ICIT 2005 Proceedings of IEEE International Conference on Industrial Technology, pp 1269–1273
4. Dua DS, Liua YD, Guoa XG, Yamazakia K, Fujishimab M (2010) An accurate adaptive NURBS curve interpolator with real-time flexible acceleration/deceleration control. Robot Cim-Int Manuf 26(4):273–281. doi:10.1016/j.rcim.2009.09.001
5. Erkorkmaz K, Altintas Y (2001) High speed CNC system design. Part I: jerk limited trajectory generation and quintic spline interpolation. Int J Mach Tools Manuf 41(9):1323–1345. doi:10.1016/S0890-6955(01)00002-5
6. Jeon JW, Ha YY (2000) A generalized approach for the acceleration and deceleration of industrial robots and CNC machine tools. IEEE Trans Ind Electr 47(1):133–139. doi:10.1109/41.824135
7. Jun H, Xiao LJ, Wang YH, Wu ZY (2006) An optimal feedrate model and solution algorithm for a high-speed machine of small line blocks with look-ahead. Int J Adv Manuf Technol 28:930–935. doi:10.1007/s00170-004-1884-2
8. Lee CS (2010) Generation of velocity profiles with speed limit of each axis for high-speed machining using look-ahead buffer. Int J Precis Eng Manuf 11(2):201–208. doi:10.1007/s12541-010-0023-2
9. Lin MT, Tsai MS, Yau HT (2007) Development of a dynamics-based NURBS interpolator with real-time look-ahead algorithm. Int J Mach Tools Manuf 47(15):2246–2262. doi:10.1016/j.ijmachtools.2007.06.005
10. Luo FY, Zhou YF, Yin J (2007) A universal velocity profile generation approach for high-speed machining of small line segments with look-ahead. Int J Adv Manuf Technol 35:505–518. doi:10.1007/s00170-006-0735-8
11. Shi C, Ye PQ (2011) The look-ahead function-based interpolation algorithm for continuous micro-line trajectories. Int J Adv Manuf Technol 54:649–668. doi:10.1007/s00170-010-2975-x
12. Shipitalni M, Koren Y, Lo CC (1994) Real-time curve interpolators. Comput-Aided Des 26(11):832–838
13. Tsai MS, Nien HW, Yau HT (2008) Development of an integrated look-ahead dynamics-based NURBS interpolator for high precision machinery. Comput-Aided Des 40(5):554–566. doi:10.1016/j.cad.2008.01.015
14. Wang L, Cao JF, Li YQ (2010) Speed optimization control method of smooth motion for high-speed CNC machine tools. Int J Adv Manuf Technol 49:313–325. doi:10.1007/s00170-009-2383-2
15. Wang FC, Wright PK (1998) Open architecture controllers for machine tools, part 2: a real time quintic spline interpolator. ASME Trans J Manuf Sci Eng 120:425–432
16. Yau HT, Wang JB (2007) Fast Bezier interpolator with real-time look ahead function for high-accuracy machining. Int J Mach Tools Manuf 47(10):1518–1529. doi:10.1016/j.ijmachtools.2006.11.010
17. Yau HT, Wang JB, Chen WC (2005) Development and implementation for real-time lookahead interpolator by using Bezier curve to fit CNC continuous short blocks. In: ICM '05 Proceedings of the IEEE International Conference on Mechatronics, pp 78–83
18. Ye PQ, Shi C, Yang KM, Lv Q (2008) Interpolation of continuous micro line segment trajectories based on look-ahead algorithm in high-speed machining. Int J Adv Manuf Technol 37:881–897. doi:10.1007/s00170-007-1041-9
19. Zheng KJ, Cheng L (2008) Adaptive s-curve acceleration/deceleration control method. In: WCICA 2008 proceedings of 7th World Congress on Intelligent Control and Automation, pp 2752–2756